

ORIGINAL RESEARCH

Endoplasmic Reticulum Selective Autophagy Alleviates Anthracycline-Induced Cardiotoxicity



Shun Nakagama, MD,^a Yasuhiro Maejima, MD, PhD,^a Qintao Fan, MD,^a Yuka Shiheido-Watanabe, DDS, PhD,^a Natsuko Tamura, MD, PhD,^a Kensuke Ihara, MD, PhD,^{a,b} Tetsuo Sasano, MD, PhD^a

ABSTRACT

BACKGROUND The administration of anthracycline drugs induces progressive and dose-related cardiac damage through several cytotoxic mechanisms, including endoplasmic reticulum (ER) stress. The unfolded protein response plays a crucial role for mitigating misfolded protein accumulation induced by excessive ER stress.

OBJECTIVES We aimed to clarify whether endoplasmic reticulum-selective autophagy machinery (ER-phagy) serves as an alternative system to protect cardiomyocytes from ER stress caused by anthracycline drugs.

METHODS Primary cultured cardiomyocytes, H9c2 cell lines, and cardiomyocyte-specific transgenic mice, all expressing ss-RFP-GFP-KDEL proteins, were used as ER-phagy reporter models. We generated loss-of-function models using RNA interference or gene-trap mutagenesis techniques. We assessed phenotypes and molecular signaling pathways using immunoblotting, quantitative polymerase chain reaction, cell viability assays, immunocytochemical and histopathological analyses, and cardiac ultrasonography.

RESULTS The administration of doxorubicin (Dox) activated ER-phagy in ss-RFP-GFP-KDEL-transduced cardiomyocytes. In addition, Dox-induced cardiomyopathy models of ER-phagy reporter mice showed marked activation of ER-phagy in the myocardium compared to those of saline-treated mice. Quantitative polymerase chain reaction analyses revealed that Dox enhanced the expression of cell-cycle progression gene 1 (CCPG1), one of the ER-phagy receptors, in H9c2 cells. Ablation of CCPG1 in H9c2 cells resulted in the reduced ER-phagy activity, accumulation of proapoptotic proteins, and deterioration of cell survival against Dox administration. CCPG1-hypomorphic mice developed more severe deterioration in systolic function in response to Dox compared to wild-type mice.

CONCLUSIONS Our findings highlight a compensatory role of CCPG1-driven ER-phagy in reducing Dox toxicity. With further study, ER-phagy may be a potential therapeutic target to mitigate Dox-induced cardiomyopathy. (J Am Coll Cardiol CardioOnc 2023;5:656–670) © 2023 The Authors. Published by Elsevier on behalf of the American College of Cardiology Foundation. This is an open access article under the CC BY-NC-ND license (<http://creativecommons.org/licenses/by-nc-nd/4.0/>).

From the ^aDepartment of Cardiovascular Medicine, Graduate School of Medical and Dental Sciences, Tokyo Medical and Dental University, Tokyo, Japan; and the ^bDepartment of Bio-informational Pharmacology, Medical Research Institute, Tokyo Medical and Dental University, Tokyo, Japan.

The authors attest they are in compliance with human studies committees and animal welfare regulations of the authors' institutions and Food and Drug Administration guidelines, including patient consent where appropriate. For more information, visit the [Author Center](#).

Manuscript received January 19, 2023; revised manuscript received May 9, 2023, accepted May 15, 2023.

Autophagy is a well-conserved intracellular degradation system on which a double-membrane structure (ie, phagophore) engulfs the cytosolic components to form an autophagosome and delivers them to lysosomes.¹ In contrast to “bulk autophagy,” a nonspecific degradation form of autophagy that mainly produces energetic resources, “selective autophagy” targets specific components for their clearance.² Accumulating evidence suggests an important contributory role of autophagy machinery, particularly mitochondria-selective autophagy (mitophagy), in the development of heart failure (HF).³⁻⁵

Regarding protein synthesis and calcium handling, the endoplasmic reticulum (ER) plays an important role in cardiomyocytes. Because severe ER impairment causes various cardiovascular diseases, including HF,^{6,7} there is an intracellular mechanism for reducing ER damage. The unfolded protein response (UPR) pathway suppresses the general protein synthesis, upregulates UPR-related gene expression, and degrades excessive proteins through ER-associated degradation, consequently reducing ER stress in response to the accumulating misfolded proteins for maintaining ER homeostasis.⁸ Besides UPR activation, an autophagic ER processing system termed endoplasmic reticulum-selective autophagy (ER-phagy) plays a protective role against ER stress in eukaryotic cells by mediating damaged ER degradation.^{9,10} However, despite the potentially beneficial function of ER-phagy in cardiomyocytes, only a few reports show the presence or the function of ER-phagy in cardiomyocytes because there is no reliable ER-phagy monitoring system.^{11,12} Therefore, the potential cardioprotective role of ER-phagy and its molecular mechanisms are yet to be elucidated.

Anthracyclines, including doxorubicin (Dox), are extensively used in the treatment of various types of neoplasms. However, a number of anthracycline-treated patients suffer adverse side effects because of the progressive and dose-related cardiotoxicity of these drugs, which has the potential to result in refractory HF.¹³ A growing body of evidence suggests that several cytotoxic mechanisms, including excessive generation of free radicals from mitochondria and iron-induced toxicity, mediate anthracycline-induced cardiotoxicity.¹⁴⁻¹⁶ Additionally, previous studies have shown that Dox-induced cardiac dysfunction is partly mediated by severe ER stress in cardiomyocytes.¹⁷ However, the exact mechanism through which Dox exerts this cardiotoxic effect by worsening ER stress is yet to be elucidated.

In this study, we aimed to test the hypothesis that ER-phagy contributes a cardioprotective role in

mitigating Dox cardiotoxicity by maintaining ER homeostasis. To this end, we developed monitoring systems of ER-phagy in cardiomyocytes in both in vitro and in vivo experimental models. Furthermore, using the Dox-induced cardiomyopathy models, we revealed that ER-phagy exerted its cardioprotective role through the signaling pathway of CCPG1, one of the ER-phagy receptor molecules.

METHODS

The methods are further detailed in the [Supplemental Methods](#).

CELLS AND REAGENTS. H9c2 cells, human embryonic kidney cells 293 (HEK293), and human embryonic kidney cells 293T (HEK293T) were purchased from American Type Culture Collection and cultured in Dulbecco’s modified Eagle’s medium (Sigma-Aldrich). For the primary cultures of neonatal rat ventricular cardiomyocytes (NRVCs), we excised ventricles from 0- to 1-day-old Wistar rats and isolated cardiomyocytes following the manufacturer’s guidance of the Pierce Primary Cardiomyocyte Isolation Kit (Thermo Fisher Scientific). Dox (Cayman Chemical) was added to the medium for 24 hours at a concentration of 1 μmol/L in all experiments unless otherwise stated to evaluate its effect on cardiomyocytes. For the starvation experiment, cells were incubated in Earle’s Balanced Salt Solution (EBSS) (Gibco).

EXPERIMENTAL ANIMAL MODELS. Mice were fed with standard chow diet and water and kept in a room at 22 to 25 °C and 40% to 60%. For echocardiograms, animals were anesthetized with isoflurane (3%). Mice were sacrificed by cervical dislocation. Both male and female mice of 8 to 10 weeks old were assessed in all experiments. Cardiomyocyte-specific ER-phagy reporter mice (Tg-tf-KDEL mice) were generated by microinjection of the plasmid to embryonic stem cell from a C57BL6/N background. To generate the CCPG1 hypomorphic mice (*Ccp1*^{GT/GT} mice), we purchased frozen mouse sperm of *Ccp1*^{TM1b(EUCOMM)Hmgu} on a C57BL6/N background from the Institute of Experimental Genetics, Helmholtz Zentrum München. *Ccp1*^{GT/GT} and control wild-type mice were obtained by crossing heterozygote littermates. To induce Dox cardiomyopathy mouse models, we injected the mice with Dox (5 mg/kg) intraperitoneally once a week for 4 weeks (cumulative dose of 20 mg/kg) and analyzed them after the indicated period. All animal experimental procedures complied with a protocol approved by the Tokyo Medical and Dental University Guide for the Care and Use of Laboratory Animals

ABBREVIATIONS AND ACRONYMS

CCPG1	= cell-cycle progression gene 1
Dox	= doxorubicin
ER	= endoplasmic reticulum
GFP	= green fluorescent protein
HF	= heart failure
NRVC	= neonatal rat ventricular cardiomyocyte
RFP	= red fluorescent protein
TBK1	= TANK-binding kinase 1
UPR	= unfolded protein response

(permission number: A2023-108C, 2022-096C, G2019-004C7, G2019-038C4) and *The Guide for the Care and Use of Laboratory Animals* published by the US National Institutes of Health.

PLASMIDS. The pCW57.1-CMV-ssRFPGFPKDEL plasmid was a gift from Dr N. Mizushima. Green fluorescent protein (GFP), ss-RFP-GFP-KDEL, and CCPG1 complementary DNA were inserted into various vectors via polymerase chain reaction-mediated mutagenesis. Plasmids containing the GFP-CCPG1 sequence and small hairpin RNA sequences were purchased from VectorBuilder Biosciences Inc.

PREPARATION OF ADENOVIRUS AND LENTIVIRUS. We constructed and propagated recombinant adenovirus and lentivirus to deliver genetic material into cells. The lentiviral titer was assessed using the p24 Rapid Titer Kit (Takara Bio).

IMMUNOBLOTTING. H9c2 cells and heart tissue homogenates were lysed with radio-immunoprecipitation assay buffer. Samples were then separated by polyacrylamide gels and transferred onto polyvinylidene fluoride or nitrocellulose membranes. The transferred membranes were probed overnight with a primary antibody and then with a secondary antibody before visualizing the blots using a iBright CL1500 Instrument (Thermo Fisher Scientific).

CONFOCAL FLUORESCENCE MICROSCOPY. Live H9c2 cells were visualized using a confocal fluorescence microscope with specific laser wavelengths, whereas in vivo heart tissue was fixed, mounted with DAPI Fluoromount-G (Cosmo Bio), and visualized with a cryostat. Immunohistochemical staining was performed, and images were captured using a TCS SP8 microscope (Leica).

SERIAL SECTION ARRAY TOMOGRAPHY. Fresh NRVCs were fixed, embedded in epoxy resin, and cut into ultrathin sections. Images were captured using a JSM-7900F microscope (JEOL).

IMMUNOELECTRON MICROSCOPY. Fixed NRVCs were permeabilized with block solution; incubated with anti-KDEL, anti-GFP, and anti-red fluorescent protein (RFP) antibodies conjugated with Nanogold particles (Nanoprobes); and visualized using the pre-embedding silver enhancement immunogold method and H7100/XR81 (Hitachi).

TIME-LAPSE FLUORESCENCE MICROSCOPY. Live H9c2 cells were treated and visualized on a fluorescence microscope per the manufacturer's guidelines in a time lapse of 1 hour.

QUANTITATIVE REVERSE TRANSCRIPTION POLYMERASE CHAIN REACTION. RNA was extracted from cells or heart tissue, synthesized into complementary DNA,

and analyzed using quantitative polymerase chain reaction using THUNDERBIRD SYBR qPCR Mix (TOYOBO). [Supplemental Table 1](#) lists the polymerase chain reaction primers.

CELL VIABILITY ASSAY/TERMINAL DEOXY-NUCLEOTIDYL TRANSFERASE-MEDIATED dUTP NICK END-LABELING ASSAY. H9c2 cells were transduced with lentiviral small hairpin RNA and exposed to Dulbecco's modified Eagle's medium or Dox. Then, cell viability (Cell Counting Kit-8; Dojindo Molecular Technology) assays or terminal deoxy-nucleotidyl transferase-mediated dUTP nick end-labeling assays were performed.

ASSESSMENT OF CARDIAC FUNCTION. Cardiac function of mice was assessed by echocardiography. M-mode images were used to measure parameters of left ventricular diameter, thickness, and function.

HISTOPATHOLOGICAL ANALYSIS. Mice hearts were imaged with staining, and the fibrosis area was calculated using ImageJ (National Institutes of Health).

ON-BEADS MASS SPECTROMETRY ANALYSIS. HEK293 cells were transfected with plasmid encoding GFP or GFP-CCPG1. Lysates were harvested and mixed with anti-GFP mab-Magnetic Beads (MBL). On-beads liquid chromatography/tandem mass spectrometry was performed.

PULL-DOWN ASSAY. Myc-tagged CCPG1 protein was expressed in vitro and mixed with TANK-binding kinase 1 (TBK1) protein. Magnetic beads were used for immunoprecipitation followed by immunoblotting.

STATISTICAL ANALYSIS. Data are presented as the mean \pm SEM. Normally distributed data were analyzed using the unpaired Student's *t*-test for comparing 2 groups or 1-way analysis of variance for comparing >2 groups followed by a post hoc Tukey-Kramer test for multiple pairwise comparisons. Otherwise, the Wilcoxon rank sum or Kruskal-Wallis test was used for comparing 2 or >2 groups. Normality of the data was checked using a Q-Q plot and the Shapiro-Wilk test. A *P* value of 0.05 was considered as a threshold of statistical significance. All statistical analyses were performed using JMP 15 (SAS Institute Inc).

RESULTS

ER-PHAGY REPORTER PROTEIN ENABLED VISUALIZING THE DEGRADATION OF ER FRAGMENTS IN CARDIOMYOCYTES. To assess the dynamic state of ER-phagy in cardiomyocytes, we attempted to develop a monitoring system of ER-phagy. To this end, we used a fluorescent probe encoding ss-RFP-GFP-KDEL sequence, an N-terminal ER signal sequence followed by tandem fluorescence

sequences, and an ER retention signal¹⁸ (Supplemental Figure 1A). This fluorescent probe enabled us to visualize the status of ER-phagy activation by expressing the reporter protein in the cells. Specifically, the degree of ER-phagy positively correlated with the amount of a single RFP signal. Once ER-phagy was activated, the reporter proteins were engulfed in autophagosomes with the ER fragments, and the linker between RFP and GFP was cleaved into 2 fragments by lysosomal enzymes in the autolysosomes. Although the GFP-containing fragment was easily degraded by lysosomal enzymes, thus contributing to a decrease in GFP fluorescence, the RFP-containing fragment required more time to be processed because of its acid-resistant nature. Accordingly, the activity of ER-phagy can be monitored by quantifying such residual RFP signals.

We transduced NRVCs with lentivirus harboring the ss-RFP-GFP-KDEL sequence (Supplemental Figure 1B). Amino acid deprivation by substituting culture medium with Earle's Balanced Salt Solution caused a significant increase of the RFP signals in these NRVCs (Figures 1A and 1B), suggesting that ss-RFP-GFP-KDEL probes worked properly in cultured primary cardiomyocytes. Then, to establish a passable in vitro model, we developed an ER-phagy-reporter-H9c2 cell line (tf-H9c2 cell), which stably expressed this reporter sequence by transducing the lentivirus harboring ss-RFP-GFP-KDEL sequence with antibiotic selection. Amino acid deprivation showed a significant increase in RFP signals in the tf-H9c2 cells (Supplemental Figures 1C and 1D). This increase in RFP signals was negated by bafilomycin A1, a reagent to block lysosomal acidification and autophagosome-lysosomal fusion (Supplemental Figure 1D). This result, along with the immunoelectron microscopic images showing that the existence of RFP and GFP signals exist in the autophagosome-like structures (Supplemental Figure 2A), suggests that the degradation of reporter proteins occurs through autophagy machinery. Treatment with dithiothreitol, a potent ER stress inducer, also facilitated the increase in RFP signals in tf-H9c2 cells (Supplemental Figure 2B).

Additionally, we generated a cardiac-specific ER-phagy reporter transgenic mouse (Tg-tf-KDEL mouse) with the ss-RFP-GFP-KDEL reporter sequence encoded by an alpha myosin heavy chain promoter (Supplemental Figures 3A and 3B). Immunoblot and fluorescent histopathological examinations showed that the reporter protein properly expressed in the heart tissues and localized in the ER compartment of the Tg-tf-KDEL mice (Figure 1C, Supplemental Figure 3C). Furthermore, immunoblot analyses using

heart lysates from the Tg-tf-KDEL mice with or without 48-hour starvation revealed increased RFP signals (Figures 1D and 1E). These reporter models could be used both in vitro and in vivo to monitor the status of ER-phagy in cardiomyocytes.

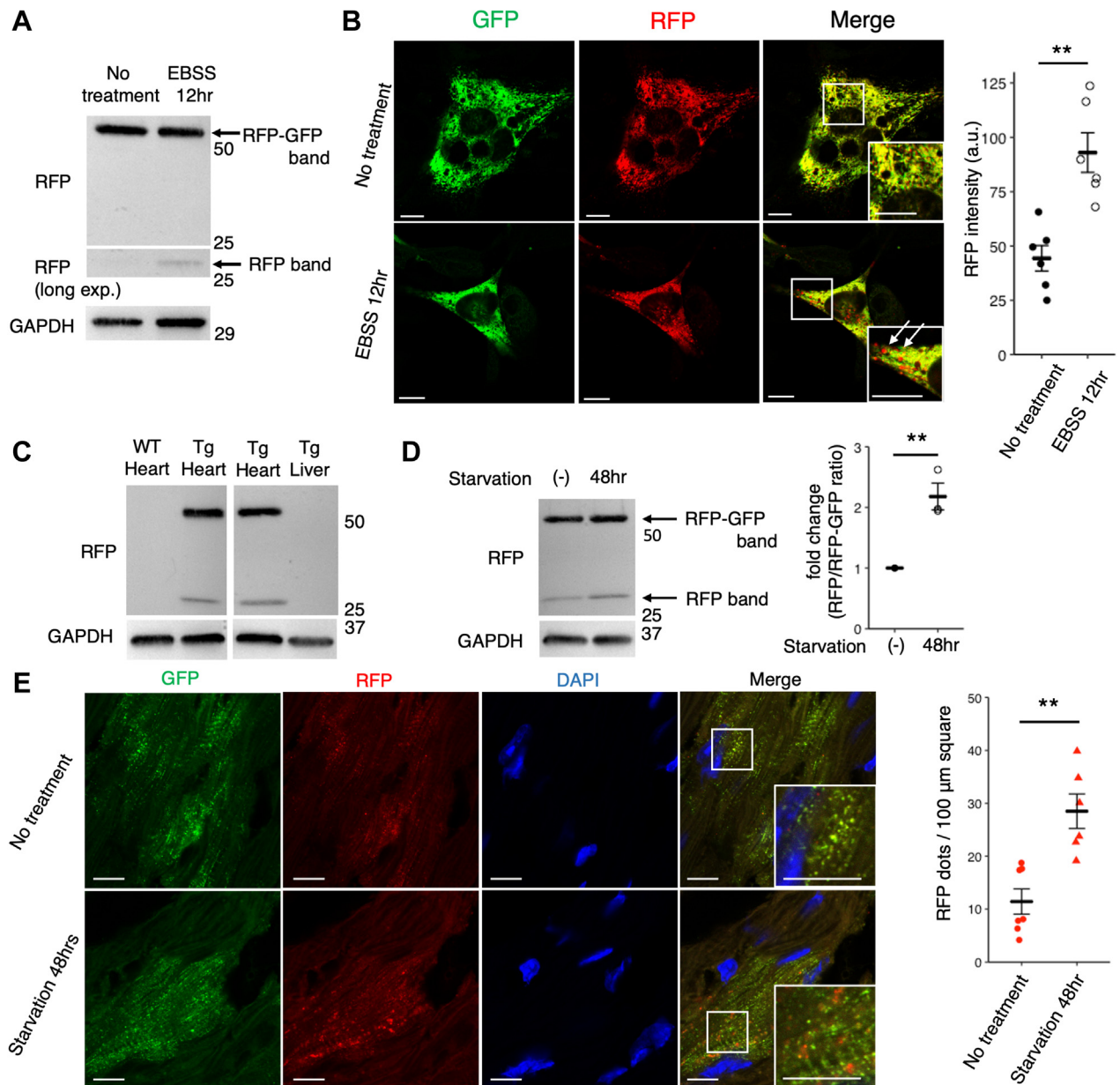
DOXORUBICIN MARKEDLY INDUCED ER-PHAGY IN CARDIOMYOCYTES.

To examine the effect of Dox on ER stress and autophagosome formation in cardiomyocytes, we first confirmed that Dox promoted ER stress signals, as evidenced by CHOP protein accumulation and phosphorylation of eIF2 α (Supplemental Figure 4A). We also observed an accumulation of the lipidated form of LC3 (LC3-II), known as an autophagosome marker, in Dox-treated cells (Supplemental Figure 4B). Additionally, we recorded a significant increase in the number of GFP-positive puncta in Dox-treated H9c2 cells expressing GFP-LC3 (Supplemental Fig. 4C). Interestingly, serial section array tomography analyses of Dox-treated NRVCs revealed autophagosomes that engulfed the ER fragment-like structure (Supplemental Figure 4D), which was not observed in nontreated NRVCs (data not shown). The sequestration of ER fragments by autophagosome was also observed by the immunoelectron microscopic analyses (Supplemental Figure 4E). These results implied that ER-phagy could be activated by Dox exposure. To test our hypothesis, we evaluated the effect of Dox on ER-phagy in cardiomyocytes using tf-H9c2 cells. We found that Dox treatment resulted in a significant increase in the RFP signals in tf-H9c2 cells (Figures 2A and 2B), suggesting that Dox induced ER-phagy. Furthermore, time-lapse microscopic analyses enabled us to capture the decisive moment of ER-phagy, indicated as the conversion of a yellow dot to a red dot along the time course (Figure 2C, Video 1).

To determine the effect of Dox on ER-phagy in animal models, we administered Dox or normal saline intraperitoneally to the Tg-tf-KDEL mice (Supplemental Figure 4F). Immunoblot analyses of their heart lysates showed a significant increase in RFP fragments in Dox-treated mice compared with those in the untreated mice (Figure 2D). Additionally, fluorescent histopathologic analysis of heart tissue sections from Tg-tf-KDEL mice demonstrated that treatment with Dox significantly increased RFP-positive puncta, suggesting that ER-phagy flux was activated in Dox-treated mice (Figure 2E). These results indicate that treatment with Dox can provoke ER-phagy in cardiomyocytes both in vitro and in vivo.

CCPG1 IS A CRITICAL INDUCER OF THE ER STRESS-ASSOCIATED ER-PHAGY. Additionally, to elucidate the underlying molecular mechanism that

FIGURE 1 Monitoring Assay Systems for Endoplasmic Reticulum-Phagy in Cardiomyocytes

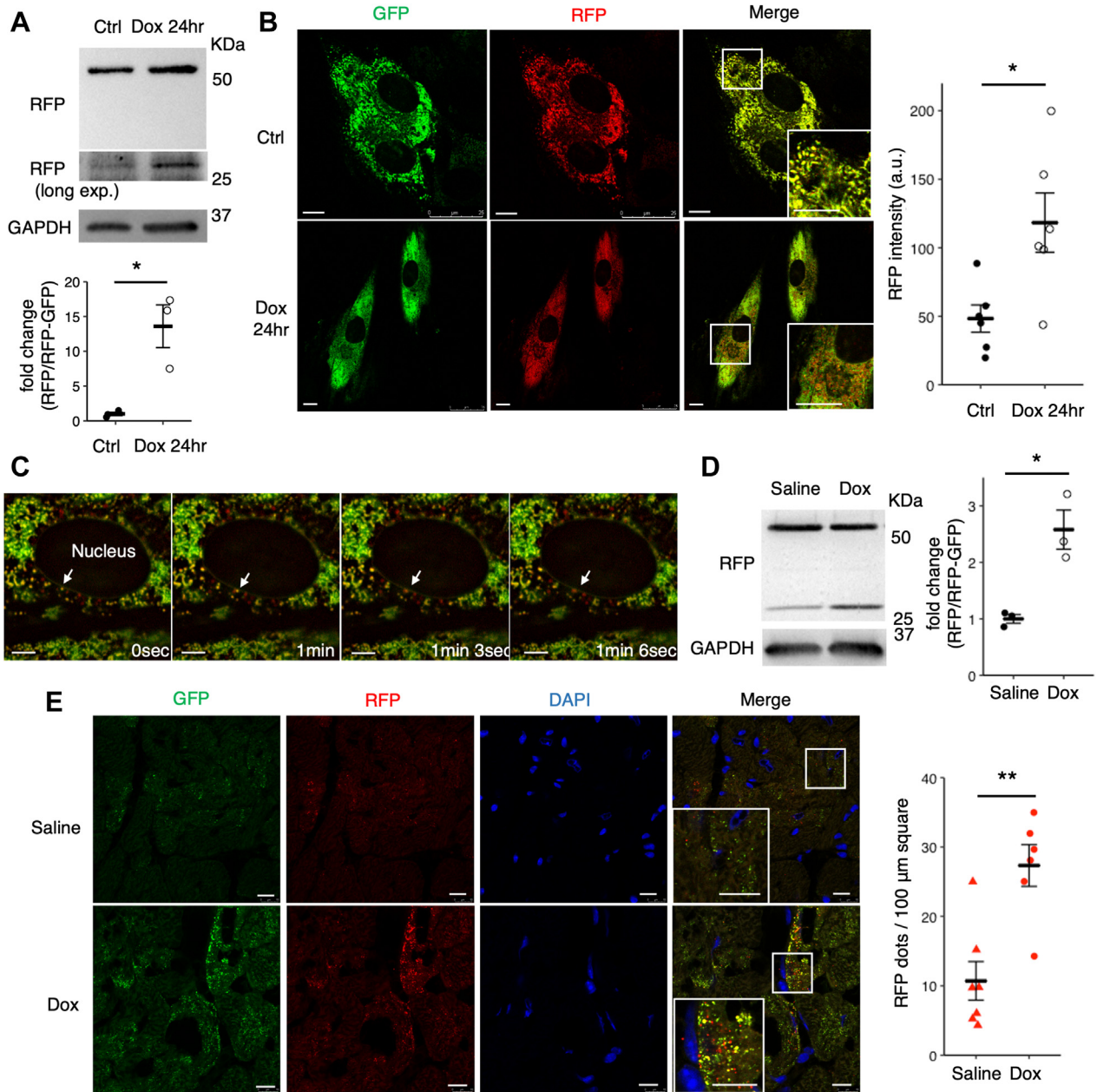


(A) Western blotting was performed after indicated treatments on neonatal rat ventricular cardiomyocytes (NRVCs) expressing endoplasmic reticulum-phagy reporter proteins. The RFP-GFP band represents the total reporter protein, whereas the RFP band represents the digested fragment. (B) The same NRVCs prepared in **Figure 1A** were visualized on confocal microscopy. The intensity of digest RFP signals (arrows) were calculated. The scale bar represents 10 μm ($n = 6$, mean \pm SEM, $^{**}P < 0.01$, t -test). (C) Western blotting of homogenized heart or liver tissue of wild-type and Tg-tf-KDEL mice. (D) Western blotting of homogenized heart tissue of Tg-tf-KDEL mice. Mice were fed normally or starved (for 48 hours) before sacrifice ($n = 3$, mean \pm SEM, $^{**}P < 0.01$, t -test). (E) Frozen heart sections from the same mice in **Figure 1D** were visualized on confocal microscopy. RFP (red) puncta per 100 μm^2 are compared. The scale bar represents 10 μm ($n = 6$, mean \pm SEM, $^{**}P < 0.01$, t -test). EBSS = Earle's balanced salt solution; GAPDH = glyceraldehyde 3-phosphate dehydrogenase; RFP-GFP = red fluorescent protein - green fluorescent protein; Tg = transgenic; WT = wild-type.

activated ER-phagy in cardiomyocytes, we evaluated the effect of Dox on the expression levels of ER membrane proteins that had been reported to regulate ER-phagy, namely TEX264, FAM134B, ATL3,

SEC62, and CCPG1 (**Supplemental Figure 5A**)^{11,18-22} in H9c2 cells. We found that CCPG1, TEX264, and Sec62 were significantly upregulated in response to Dox administration (**Figure 3A**). A recent study revealed

FIGURE 2 Dox Strongly Induces Endoplasmic Reticulum-Phagy

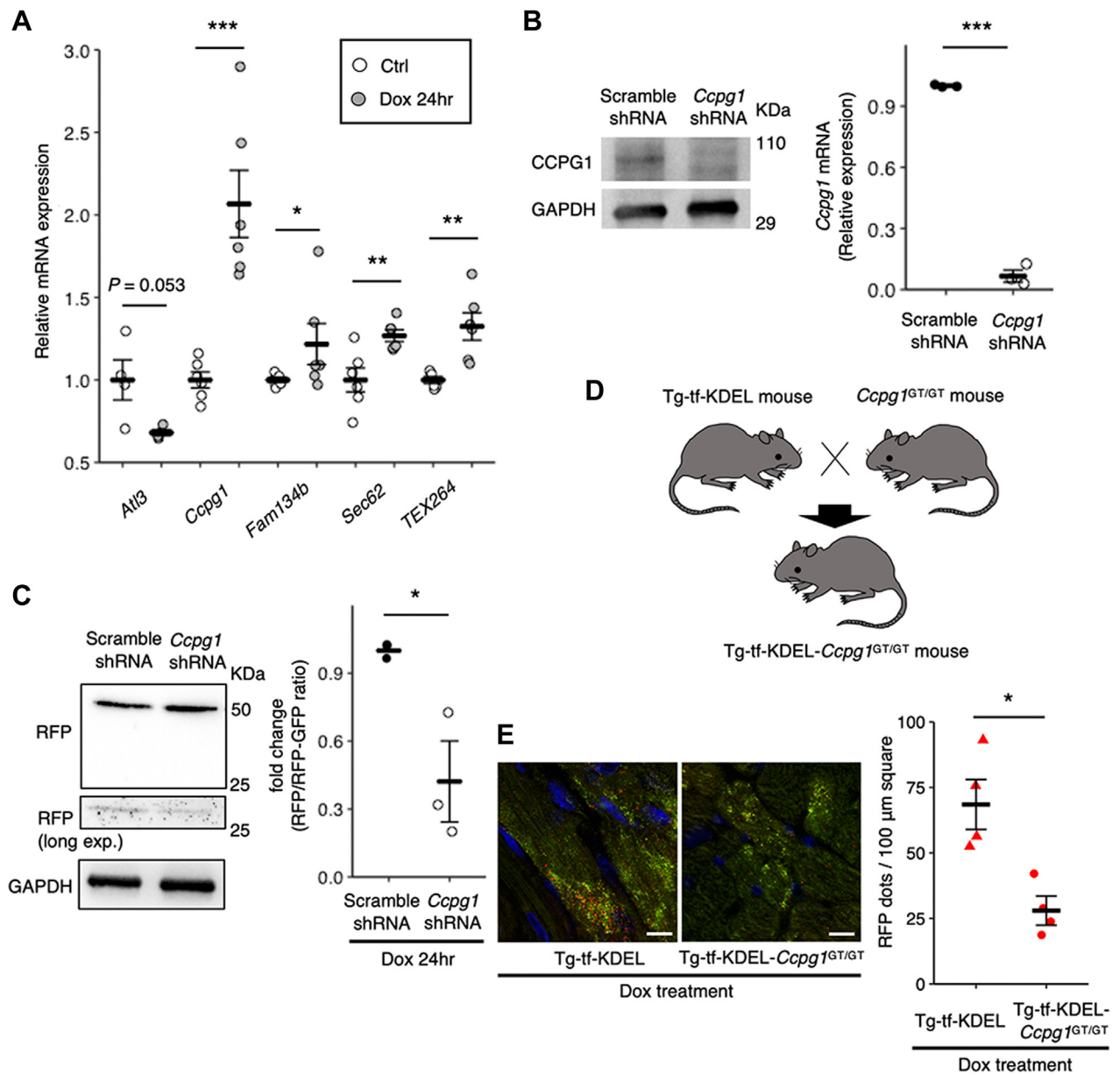


(A) Western blotting of tf-H9c2 cells treated with or without doxorubicin (Dox) (1 μmol/L for 24 h) (n = 4, mean ± SEM, *P < 0.05, t-test). (B) The same tf-H9c2 cells prepared in Figure 2A were visualized, and RFP intensity was calculated. The scale bar represents 10 μm (n = 6, mean ± SEM, *P < 0.05, t-test). (C) Live tf-H9c2 cells treated with Dox (1 μmol/L) were monitored on fluorescence microscopy. A set of time-lapse images is shown. The white arrow points to the same punctum, the color of which changes from yellow to red in 1 minute 3 seconds. The scale bar represents 5 μm. (D) Western blotting of homogenized heart tissue of Tg-tf-KDEL mice with indicated treatment (n = 3, mean ± SEM, *P < 0.05, t-test). (E) Frozen heart sections from saline- or Dox-treated Tg-tf-KDEL mice were visualized. RFP (red) puncta per 100 μm square were counted. The scale bar represents 10 μm (n = 7, mean ± SEM, **P < 0.01, t-test). Abbreviations as in Figure 1.

that CCPG1 is the protein responsible for initiating ER-phagy under ER stress conditions in mammalian cells.¹⁰ As described, Dox exerts cardiotoxicity partly by inducing ER stress in cardiomyocytes.¹⁷ These

observations led us to hypothesize that CCPG1 may enhance ER-phagy to reduce the Dox-induced cardiotoxicity mediated by excessive ER stress. Therefore, to evaluate CCPG1's role in ER-phagy activity,

FIGURE 3 CCPG1 Regulated ER-Phagy Activity Induced by Dox Administration



(A) Transcripts of H9c2 cells were collected after Dox administration (1 $\mu\text{mol/L}$ for 24 hours) and the gene expressions of *Ccp1*, *Tex264*, *Fam134b*, *Sec62*, and *At13* are compared ($n = 6$, mean \pm SEM, * $P < 0.05$, ** $P < 0.01$, *** $P < 0.001$, *t*-test). (B) The expressions of cell-cycle progression gene 1 (CCPG1) protein and transcripts from tf-H9c2 cells were compared after lentiviral transduction with indicated short hairpin RNA (shRNA) ($n = 4$, mean \pm SEM, *** $P < 0.001$, *t*-test). (C) Western blotting of tf-H9c2 cells, treated with Dox (1 $\mu\text{mol/L}$ for 24 hours) after lentiviral transduction containing indicated shRNA ($n = 3$, mean \pm SEM, * $P < 0.05$, *t*-test). (D) A schematic design for generating Tg-tf-KDEL-*Ccp1*^{GT/GT} mouse. (E) A set of representative confocal microscopic images of frozen heart sections from Dox-treated Tg-tf-KDEL and Tg-tf-KDEL-*Ccp1*^{GT/GT}. Only the merged images (GFP, RFP, and 4',6-diamidino-2-phenylindole [DAPI]) are shown. RFP (red) puncta per 100 μm square are compared. The scale bar represents 10 μm ($n = 4$, mean \pm SEM, * $P < 0.05$, *t*-test). Abbreviations as in Figures 1 and 2.

we transduced a lentivirus harboring short hairpin RNA for CCPG1 (LV-sh-CCPG1) to tf-H9c2 cells (Figure 3B). The knockdown of CCPG1 by LV-sh-CCPG1 abolished the increase of the RFP signals induced by

Dox in the tf-H9c2 cells (Figure 3C), suggesting that CCPG1 could be crucial in regulating Dox-induced ER-phagy. We also confirmed that CCPG1 abolishment did not reduce the overall autophagic flux, as

assessed by the increase in the lipidated form of LC3 upon bafilomycin A1 administration (Supplemental Figure 5B). To further examine the regulatory role of CCPG1 on ER-phagy using in vivo models, we used a CCPG1 hypomorphic mice strain engineered by a gene trap strategy (*Ccpgr1^{GT/GT}* mouse), a strain well validated as a loss-of-function model of CCPG1¹⁰ (Supplemental Figure 6A). After confirming that the expression of CCPG1 is completely suppressed in *Ccpgr1^{GT/GT}* hearts (Supplemental Figures 6B and 6C), we subsequently generated bigenic mice using *Ccpgr1^{GT/GT}* and Tg-tf-KDEL mice (Tg-tf-KDEL-*Ccpgr1^{GT/GT}* mice) (Figure 3D). The RFP signals induced by Dox treatment in Tg-tf-KDEL-*Ccpgr1^{GT/GT}* hearts were significantly lower than those in Tg-tf-KDEL mice (Figure 3E). These results indicate that CCPG1 removal results in the abolition of ER-phagy triggered by Dox administration in cardiomyocytes.

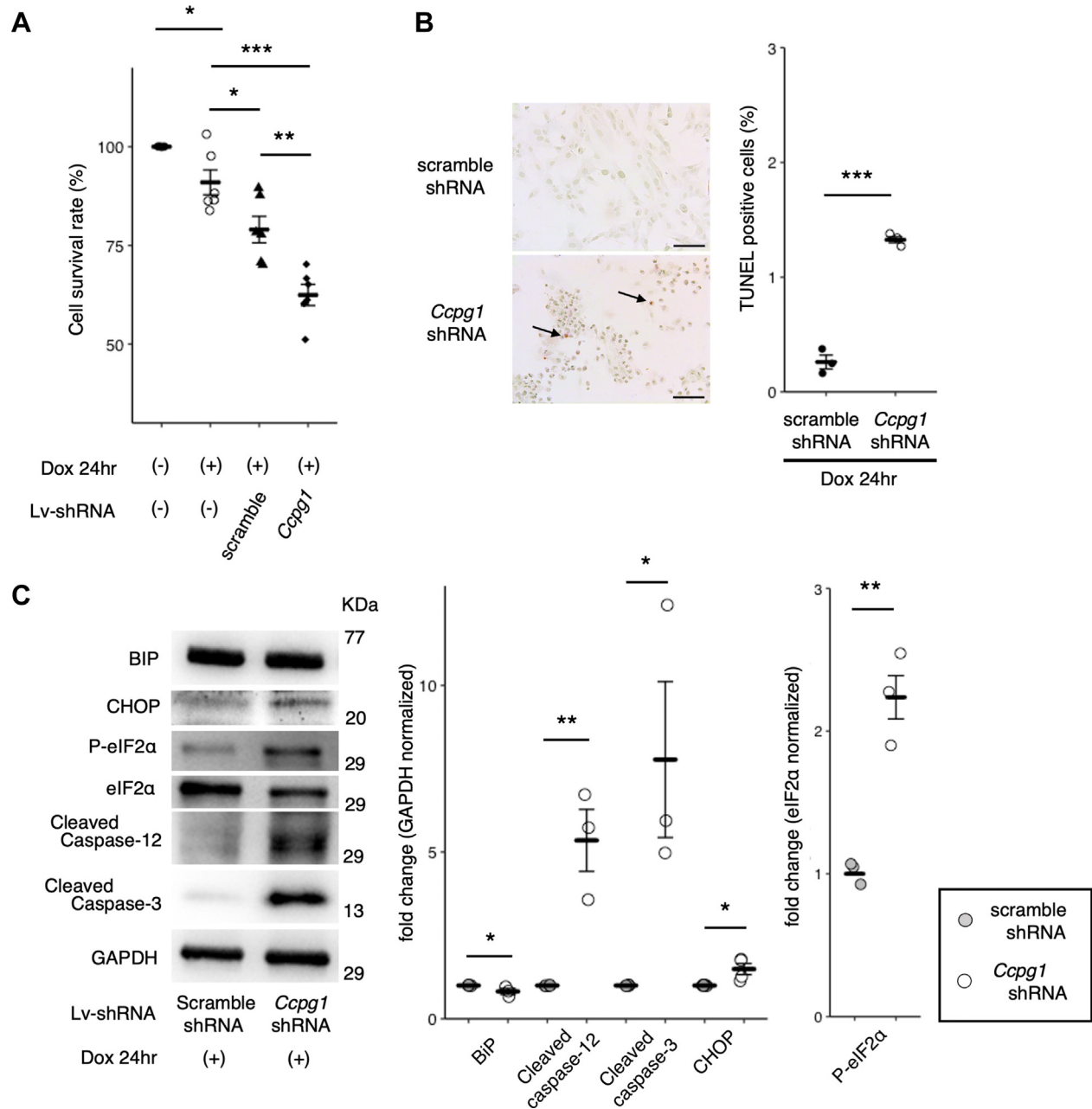
CCPG1 PLAYS A CELL PROTECTIVE ROLE BY SUPPRESSING DOX-INDUCED ER STRESS AND APOPTOTIC PATHWAY IN CARDIOMYOCYTES. Next, we addressed the functional role of CCPG1 ablation in cardiomyocytes during Dox exposure. The cell viability of Dox-treated LV-sh-CCPG1-transduced H9c2 cells was significantly reduced compared with that of LV-sh-scramble-transduced H9c2 cells (Figure 4A). The decline in cell survival observed in cells treated with Dox-alone cells indicated that the increase in ER-phagy is not sufficient to compensate the overall damage caused by Dox treatment. We next confirmed the knockdown of CCPG1-increased apoptosis in H9c2 cells, as evaluated with the terminal deoxy-nucleotidyl transferase-mediated dUTP nick end-labeling assays (Figure 4B). Furthermore, we evaluated the effect of CCPG1 removal on the expression of both ER stress- and apoptosis-associated proteins in H9c2 cells by immunoblot analyses. The levels of ER stress-associated proteins, including phosphorylated eIF2 α and CHOP, increased significantly in the Dox-treated H9c2 cells (Figure 4C). Concurrently, the levels of proapoptotic signals, including cleaved caspase-3 and caspase-12, evidently accumulated in the Dox-treated H9c2 cells (Figure 4C). The release of cytochrome c level from mitochondria to cytosol fraction was also enhanced in LV-sh-CCPG1-transduced H9c2 cells (Supplemental Figure 6D). These results indicate that CCPG1 exerts its cell-protective effects by suppressing the ER stress-mediated apoptotic pathway induced by Dox administration.

ABLATION OF CCPG1 EXACERBATES CARDIAC FUNCTION IN DOX-INDUCED CARDIOMYOPATHY ANIMAL MODELS. We examined the cardiac phenotypes of *Ccpgr1^{GT/GT}* mice to evaluate the functional

significance of CCPG1 in the hearts. At baseline, parameters of cardiac function, histologic findings, and the levels of ER stress markers of *Ccpgr1^{GT/GT}* hearts were comparable with those of wild-type hearts (Figure 5A, Supplemental Figures 7A and 7B, Supplemental Table 1). Echocardiographic examinations conducted 8 weeks after Dox treatment (Supplemental Figure 7C) indicated that the deterioration of the left ventricular systolic function was more significant in *Ccpgr1^{GT/GT}* mice than in wild-type mice (Figure 5B, Supplemental Table 2), although both mice showed decreased left ventricular systolic function along the time course (Supplemental Figure 7D). Postmortem analyses of *Ccpgr1^{GT/GT}* mice at 8 weeks after Dox treatment showed a significant increase in heart weight/body weight compared with wild-type mice (Figure 5B). Histopathologic examinations of the excised heart specimens revealed that the interstitial fibrosis of the myocardium was more prominent in the *Ccpgr1^{GT/GT}* mice than in wild-type mice (Figure 5C). Immunoblot analyses using heart lysates revealed that phosphorylated eIF2 α , an ER stress marker, was significantly upregulated in the *Ccpgr1^{GT/GT}* hearts compared with wild-type mice (Figure 5D), which were treated by Dox using a high-dose protocol (Supplemental Figure 7E). These results indicate that endogenous CCPG1 mitigates Dox-induced cardiotoxicity, possibly alleviating excessive ER stress in the hearts.

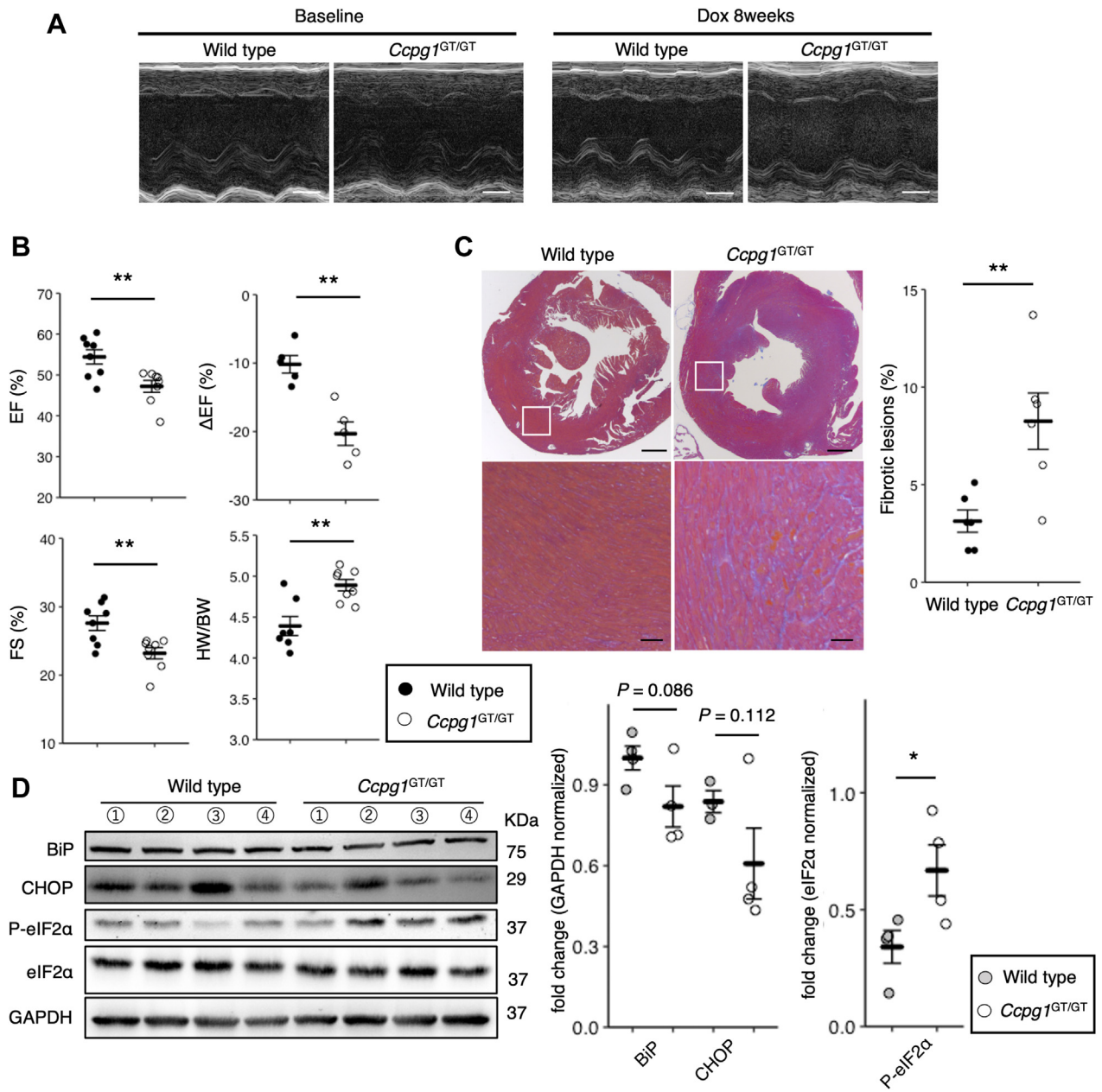
PROTEOMIC ANALYSIS REVEALED THE INTERACTION BETWEEN CCPG1 AND TANK-BINDING KINASE 1, A SERINE/THREONINE-PROTEIN KINASE. To examine the molecular mechanism of how CCPG1 mediates ER-phagy in response to excessive ER stress, we initially overexpressed CCPG1 in the tf-H9c2 cells and analyzed their phenotypic response to Dox. Consistent with a previous investigation,²³ increased expression of CCPG1 could not prevent Dox-induced cell death (Figures 6A and 6B). Consistently, the overexpression of CCPG1 could not induce RFP fragment generation in the tf-H9c2 cells (Figure 6C), indicating that the induction of ER-phagy in response to ER stress would be mediated through another specific signaling pathway independent of the CCPG1 expression level. Therefore, to examine such mechanisms, proteins that interact with CCPG1 were explored by a coimmunoprecipitation-based proteomic analysis. Lysates of HEK293 cells, in which GFP or GFP-CCPG1 was overexpressed (Figure 6D), were immunoprecipitated using the GFP antibody-attached magnetic beads (Figure 6E, Supplemental Figure 8A). Subsequently, these immunoprecipitated beads were subjected to on-beads tandem mass spectrometric analyses. We obtained the list of

FIGURE 4 Ablation of CCPG1 Prompts ER Stress-Related Apoptosis With Dox Administration



(A) The viability of H9c2 cells was assessed between 4 groups, which were treated as indicated (n = 6, mean ± SEM, *P < 0.05, **P < 0.01, ***P < 0.001, analysis of variance with the Tukey post hoc test). (B) Terminal deoxy-nucleotidyl transferase-mediated dUTP nick end-labeling (TUNEL) assay was performed on H9c2 cells, which were treated with Dox (1 μmol/L for 24 hours) after the indicated lentiviral transduction. The rate of TUNEL-positive cells (arrows) is shown. The scale bar represents 100 μm (n = 3, mean ± SEM, ***P < 0.001, t-test). (C) Lysates of H9c2 cells, prepared as in [Figure 4B](#), were immunoblotted for the indicated antibodies. The protein expressions normalized to GAPDH or e-IF2α (for phosphorylated e-IF2α) are shown (n = 3 or 4, mean ± SEM, *P < 0.05, **P < 0.01, t-test). Abbreviations as in [Figures 1 and 3](#).

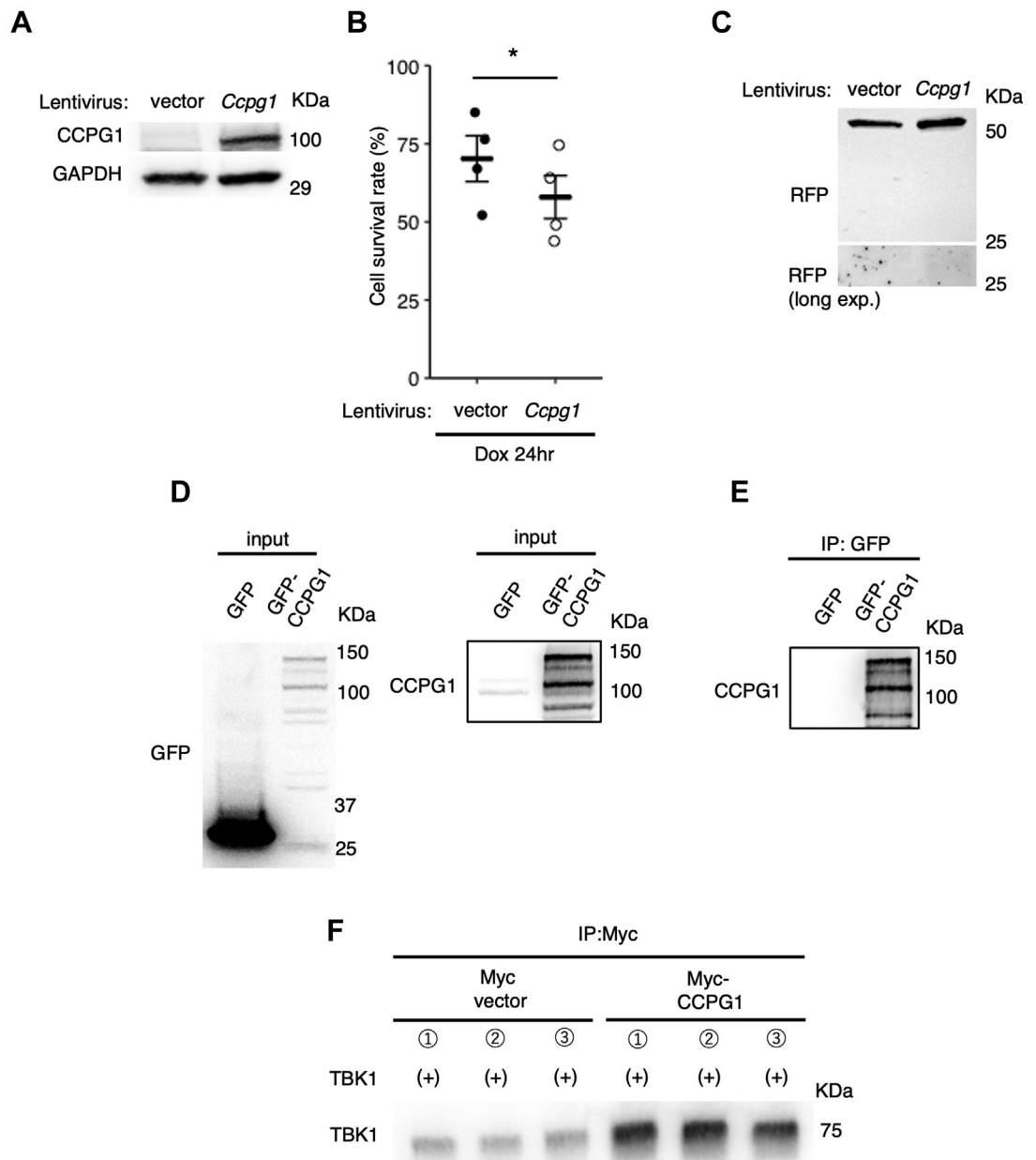
FIGURE 5 CCPG1 Hypomorphic Mice Treated With Dox Demonstrated an Exacerbated Cardiomyopathic Phenotype



(A) A representative image of echocardiography performed on wild-type and *Ccp1*^{GT/GT} mice at baseline and 8 weeks after the Dox injection. The scale bar represents 50 milliseconds. (B) Echocardiographic measurements and tissue weights, normalized to body weight, were compared (n = 8, mean ± SEM, ***P < 0.01, t-test) (C) Representative MT-stained heart sections of Dox-treated wild-type and *Ccp1*^{GT/GT} mice are shown. The scale bar represents 500 μm and 50 μm (for upper and lower images, respectively). Fibrotic lesions, calculated as the blue area divided by the whole tissue area, are compared (n = 6, mean ± SEM, ***P < 0.01, t-test). (D) Lysates of hearts from wild-type or *Ccp1*^{GT/GT} mice treated along with a high-dose Dox protocol were immunoblotted for the indicated antibodies (n = 4, mean ± SEM, *P < 0.05, t-test). BW = body weight; EF = ejection fraction; FS = fraction shortening; HW = heart weight; other abbreviations as in [Figures 1 to 3](#).

possible interactors using this unbiased, comprehensive assay system ([Supplemental Table 3](#)). Among the identified proteins, we chose selective autophagy-related proteins ([Supplemental Figure 8B](#))

and found that TBK1 is an interacting protein with CCPG1. Pull-down assays certified that TBK1 strongly interacted with myc-CCPG1 ([Figure 6F](#)). Combined with the previous findings that TBK1 is

FIGURE 6 TBK1 Physically Interacts With CCPG1

(A) Western blotting of tf-H9c2 cells transduced with CCPG1-harboring lentivirus or empty vector. (B) The tf-H9c2 cells, prepared in Figure 6A, were treated with Dox (1 $\mu\text{mol/L}$ for 24 hours). The cell survival rate after Dox treatment was compared ($n = 4$, mean \pm SEM, $*P < 0.05$, t -test) (C) Western blotting of tf-H9c2 cells prepared in Figure 6A. (D) Western blotting of HEK293 cells, which were transfected with plasmids coding GFP or GFP-CCPG1. (E) Lysates of HEK293 cells prepared in Figure 6D were immunoprecipitated with anti-GFP magnetic beads. Eluted samples from magnetic beads were immunoblotted for anti-CCPG1 antibody. (F) Pull-down assay. Recombinant TBK1, mixed with Myc or Myc-tagged CCPG1, was immunoprecipitated with Myc-tagged magnetic beads and subsequently immunoblotted for anti-TBK antibodies. An immunoblot result in triplicates is shown. For Figures 6A, 6C, 6D, and 6E, identical experiments were performed at least 3 times, and the representative images are shown. TBK1 = TANK-binding kinase 1; other abbreviations as in Figures 1 and 3.

activated under stress conditions and promotes various types of selective autophagy by phosphorylating specific cargo receptors and adaptors,²⁴⁻²⁶ these results propose that CCPG1 promotes ER-phagy, possibly through TBK1-mediated phosphorylation of ER-phagy-associated cargo receptor protein(s).

DISCUSSION

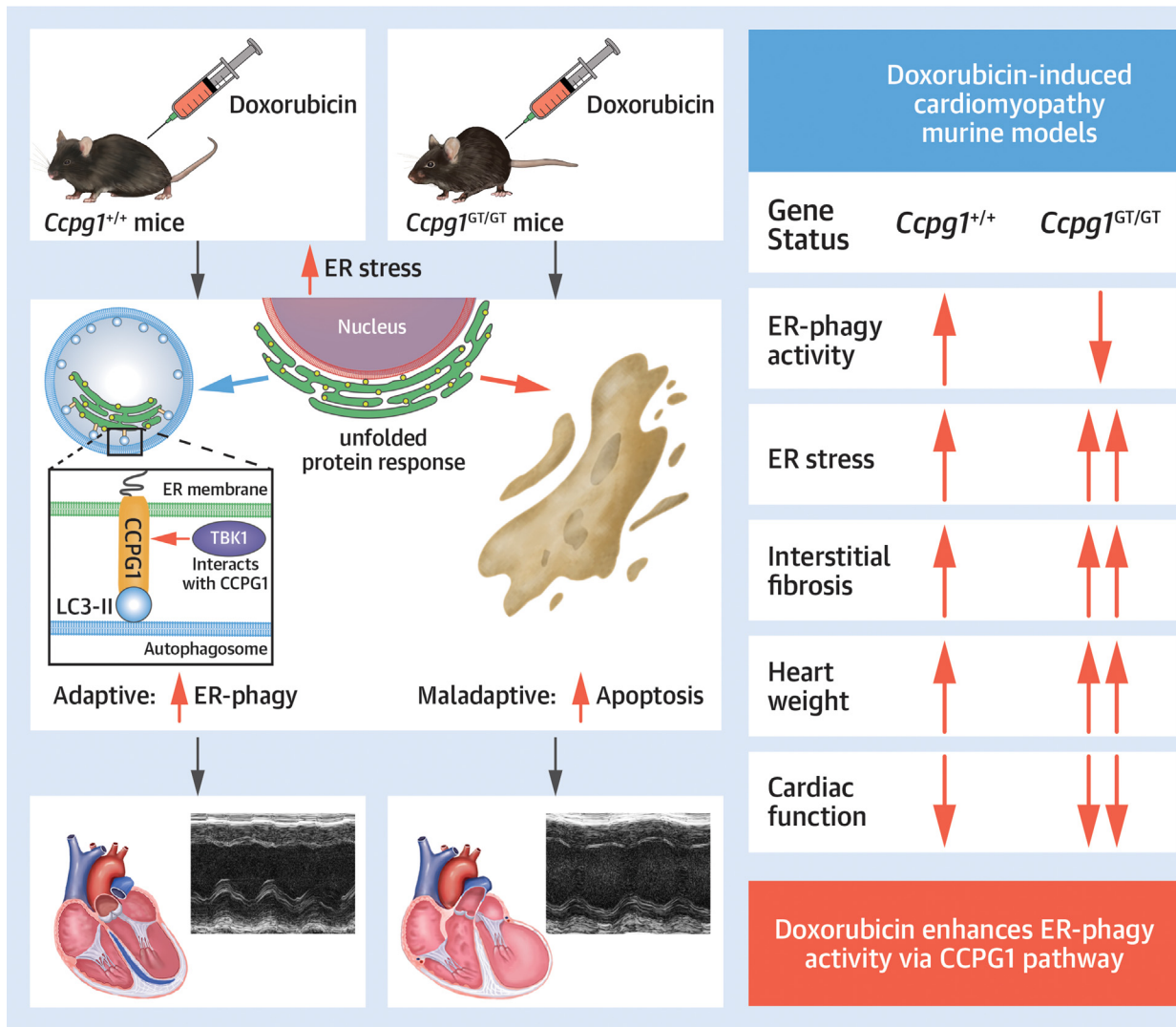
In this study, we initially established a visualization system to monitor the activity of ER-phagy in cardiomyocytes. These reporter models enabled us to evaluate and compare the amount of ER-phagy among the various samples. We also determined the critical moment of ER-phagy by time-lapse fluorescence microscopy in cardiomyocytes for the first time (Video 1). Additionally, we found that Dox treatment enhanced ER-phagy to relieve ER stress and rescue cardiomyocytes from cell death, which would otherwise occur in the absence of ER-phagy activity. Notably, CCPG1 regulates the activity of ER-phagy in a stress-dependent manner to protect cardiomyocytes from excessive ER damage and concomitant apoptosis. Finally, using murine Dox-induced cardiomyopathy models, we demonstrated the protective role of CCPG1 in promoting ER-phagy to prevent Dox-induced cardiotoxicity (Central Illustration).

Because cardiomyocytes are terminally differentiated cells, their dependency on maintenance systems for organelle homeostasis is much higher than those of other cell types.²⁷⁻²⁹ Certainly, selective autophagy plays a crucial role in maintaining organelle quality control. In the case of ER, excessive progression of ER stress results in cellular apoptosis, which leads to the development of HF.⁶ So far, UPR is known as a unique compensatory system for reducing ER stress. However, based on previous evidence,^{9,10,19} we hypothesized that alternative systems could exist so that cells can survive even if UPR fails to mitigate the ER stress. In this study, we provided novel insight to unveil the importance of ER-phagy in maintaining the intracellular homeostasis of cardiomyocytes. Our study suggests that ER-phagy activation can serve as a therapeutic option for Dox-induced cardiomyopathy. Although there is no known reagent that selectively influences ER-phagy activity, other approved medicines, including autophagy-promoting drugs such as digoxin, nondihydropyridine calcium-channel blockers, or adenosine monophosphate-activated protein kinase activators (eg, metformin),³⁰ can possibly activate ER-phagy as well, exerting its cardioprotective effect. Future studies are needed to

validate their therapeutic utility in Dox-induced cardiomyopathy.

We also attempted to explore the detailed molecular mechanism by which CCPG1 activates ER-phagy. Although the endogenous increase in CCPG1 expression is a significant hallmark of ER-phagy activation, forced overexpression of CCPG1 could not induce ER-phagy. To capitalize on the discovery of CCPG1-mediated signaling pathways that induce ER-phagy in response to ER stress, we performed comprehensive proteomic analyses and discovered TBK1 as a possible modulator of CCPG1, which would play a critical role in promoting ER-phagy. Because TBK1 is a critical regulator of several types of selective autophagy by phosphorylating specific cargo receptors, including p62/SQSTM1, OPTN, and NDP52,²⁴⁻²⁶ we hypothesized that TBK1 physically interacts with CCPG1, thereby promoting ER-phagy possibly through phosphorylating ER-phagy-associated proteins by TBK1. Although we have not obtained solid evidence that TBK1 phosphorylates CCPG1, a previous study referred to the S104 residue of CCPG1 as a possible target for phosphorylation.²⁴ Phosphorylated S104 was associated with an increase in the binding ability of CCPG1 to FIP200, 1 of the ULK complex proteins that regulate autophagy initiation.²⁴ Combined with these findings and our experimental results, TBK1 may phosphorylate CCPG1, thereby enhancing CCPG1-FIP200 interaction and facilitating the initiation of ER-phagy. Future investigations are needed to comprehensively understand the signaling pathway of ER-phagy.

STUDY LIMITATIONS. First, there is a potential limitation regarding monitoring ER-phagy. Specifically, our ER-phagy reporter assay system could not strictly differentiate the degradation of ER by ER-phagy from that caused by the coincidental bulky macroautophagy. Because ER sequestration by any autophagy pathway can increase reporter protein degradation, our reporter assay system did not precisely reflect the amount of ER-phagy. However, CCPG1 protein is dispensable in general autophagy signals. Therefore, our loss-of-function experiments of CCPG1 excluded the possibility that the increase in RFP signals caused by Dox treatment only reflected a change in bulk autophagy activity. Second, most of our *in vitro* experiments are performed using H9c2 cells. Although H9c2 cells share some similarities with cardiomyocytes, they are not considered a perfect surrogate for actual cardiomyocytes.³¹ However, we complement some of the important experiments with NRVCs, and we also validate our *in vitro* results

CENTRAL ILLUSTRATION Endoplasmic Reticulum-Selective Autophagy Protects the Heart From Doxorubicin Toxicity

Nakagama S, et al. *J Am Coll Cardiol CardioOnc.* 2023;5(5):656-670.

The administration of doxorubicin (Dox) causes cardiotoxicity by inducing excessive endoplasmic reticulum (ER) stress, which results in a failure of the unfolded protein response in cardiomyocytes. Simultaneously, Dox administration increases the expression of cell-cycle progression gene 1 (CCPG1), one of the receptors of ER-phagy, provoking ER-phagy activation, which, in turn, mitigates cardiac dysfunction by suppressing excessive ER stress-induced cardiomyocyte apoptosis. TBK1 = TANK-binding kinase 1.

with animal models. Therefore, we believe it is convincing enough to claim that the protective effect of ER-phagy takes place in cardiomyocytes. The third limitation is that our results in detecting ER stress could be incomplete. Although we demonstrated the activation of eIF2 α or CHOP, we could not show the enhancements of other ER stress markers. Our future

interests are headed toward unveiling the overall picture of all 3 ER stress pathways and toward the idea if there is a preference of which ER stress pathway is more susceptible by ER-phagy machinery. Another limitation lies in the method on inducing ER-phagy. We only investigated the function of CCPG1 and did not evaluate the ER-phagy activity,

possibly induced by other receptors, such as TEX264, FAM134B, Sec62, or ATL3. Some reports refer to TEX264 or FAM134B as other major molecules that cause ER-phagy,^{18,32} so it may be necessary to investigate the effects of these receptors. Further comprehensive investigation is needed to understand the role of ER-phagy in the cardiovascular system.

CONCLUSIONS

Our study demonstrates that ER-phagy plays a protective role in cardiomyocytes against Dox toxicity through CCPG1-mediated signaling.

ACKNOWLEDGMENTS The authors thank Noriko Tamura for her technical assistance in the preparation of histologic samples, Yuriko Sakamaki for her excellent assistance in confocal microscopy and electron microscopy, Dr Noboru Mizushima for providing us the plasmid (pCW57.1-CMV-ssRFPKDEL), and Enago for the English language review.

FUNDING SUPPORT AND AUTHOR DISCLOSURES

This work was supported by a grant from Boehringer Ingelheim, Japan Society for the Promotion of Science KAKENHI Grant-in-Aid for Scientific Research (C) (20K08399 to Dr Maejima), and Japan Science and Technology Agency for the establishment of university fellowships toward the creation of science technology innovation (JPMJSP2120 to Dr Nakagama). All authors have reported that they have no relationships relevant to the contents of this paper to disclose.

ADDRESS FOR CORRESPONDENCE: Dr Yasuhiro Maejima, Department of Cardiovascular Medicine, Graduate School of Medical and Dental Sciences, Tokyo Medical and Dental University, 1-5-45, Yushima, Bunkyo-ku, Tokyo 113-8510, Japan. E-mail: ymaejima.cvm@tmd.ac.jp.

PERSPECTIVES

COMPETENCY IN MEDICAL KNOWLEDGE: Dox-induced cardiomyopathy models of ER-phagy reporter mice showed marked activation of ER-phagy in the myocardium compared to those of saline-treated mice. Ablation of CCPG1 in H9c2 cells resulted in reduced ER-phagy activity, accumulation of proapoptotic proteins, and deterioration of cell survival against Dox administration. CCPG1-hypomorphic mice developed more severe deterioration in systolic function in response to Dox compared to wild-type mice.


TRANSLATIONAL OUTLOOK: The present study indicates the potential utility of autophagy-promoting drugs, such as digoxin; nondihydropyridine calcium-channel blockers, or adenosine monophosphate-activated protein kinase activators such as metformin as therapeutic options for doxorubicin-induced cardiomyopathy. Further translational research is needed to understand their potential therapeutic efficacy.

REFERENCES

- Mizushima N, Komatsu M. Autophagy: renovation of cells and tissues. *Cell*. 2011;147:728-741.
- Gatica D, Lahiri V, Klionsky DJ. Cargo recognition and degradation by selective autophagy. *Nat Cell Biol*. 2018;20:233-242.
- Nakai A, Yamaguchi O, Takeda T, et al. The role of autophagy in cardiomyocytes in the basal state and in response to hemodynamic stress. *Nat Med*. 2007;13:619-624.
- Maejima Y, Kyoji S, Zhai P, et al. Mst1 inhibits autophagy by promoting the interaction between Beclin1 and Bcl-2. *Nat Med*. 2013;19:1478-1488.
- Kubli DA, Zhang X, Lee Y, et al. Parkin protein deficiency exacerbates cardiac injury and reduces survival following myocardial infarction. *J Biol Chem*. 2013;288:915-926.
- Okada K, Minamino T, Tsukamoto Y, et al. Prolonged endoplasmic reticulum stress in hypertrophic and failing heart after aortic constriction: possible contribution of endoplasmic reticulum stress to cardiac myocyte apoptosis. *Circulation*. 2004;110:705-712.
- Hamada H, Suzuki M, Yuasa S, et al. Dilated cardiomyopathy caused by aberrant endoplasmic reticulum quality control in mutant KDEL receptor transgenic mice. *Mol Cell Biol*. 2004;24:8007-8017.
- Wang M, Kaufman RJ. Protein misfolding in the endoplasmic reticulum as a conduit to human disease. *Nature*. 2016;529:326-335.
- Bernales S, McDonald KL, Walter P. Autophagy counterbalances endoplasmic reticulum expansion during the unfolded protein response. *PLoS Biol*. 2006;4:e423.
- Smith MD, Harley ME, Kemp AJ, et al. CCPG1 is a non-canonical autophagy cargo receptor essential for ER-phagy and pancreatic ER proteostasis. *Dev Cell*. 2018;44:217-232.
- Perrotta I. ER-phagy in human atherosclerosis: an exploratory ultrastructural study. *Ultrastruct Pathol*. 2020;44:489-495.
- Zhang Q, Zhang X, Ding N, et al. Globular adiponectin alleviates chronic intermittent hypoxia-induced H9c2 cardiomyocytes apoptosis via ER-phagy induction. *Cell Cycle*. 2020;19:3140-3153.
- Nishi M, Wang PY, Hwang PM. Cardiotoxicity of cancer treatments: focus on anthracycline cardiomyopathy. *Arterioscler Thromb Vasc Biol*. 2021;41:2648-2660.
- Gasser A, Chen YW, Audebrand A, et al. Prokineticin receptor-1 signaling inhibits dose- and time-dependent anthracycline-induced cardiovascular toxicity via myocardial and vascular protection. *J Am Coll Cardiol CardioOnc*. 2019;1:84-102.
- Maejima Y, Adachi S, Ito H, Hirao K, Isobe M. Induction of premature senescence in cardiomyocytes by doxorubicin as a novel mechanism of myocardial damage. *Aging Cell*. 2008;7:125-136.
- Maejima Y, Adachi S, Morikawa K, Ito H, Isobe M. Nitric oxide inhibits myocardial apoptosis

- by preventing caspase-3 activity via S-nitrosylation. *J Mol Cell Cardiol.* 2005;38:163-174.
17. Fu HY, Sanada S, Matsuzaki T, et al. Chemical endoplasmic reticulum chaperone alleviates doxorubicin-induced cardiac dysfunction. *Circ Res.* 2016;118:798-809.
18. Chino H, Hatta T, Natsume T, Mizushima N. Intrinsically disordered protein TEX264 mediates ER-phagy. *Mol Cell.* 2019;74:909-921.
19. Khaminets A, Heinrich T, Mari M, et al. Regulation of endoplasmic reticulum turnover by selective autophagy. *Nature.* 2015;522:354-358.
20. Chen Q, Xiao Y, Chai P, Zheng P, Teng J, Chen J. ATL3 is a tubular ER-phagy receptor for GABARAP-mediated selective autophagy. *Curr Biol.* 2019;29:846-855.
21. An H, Ordureau A, Paulo JA, Shoemaker CJ, Denic V, Harper JW. TEX264 is an endoplasmic reticulum-resident ATG8-interacting protein critical for ER remodeling during nutrient stress. *Mol Cell.* 2019;74:891-908.
22. Fumagalli F, Noack J, Bergmann TJ, et al. Translocon component Sec62 acts in endoplasmic reticulum turnover during stress recovery. *Nat Cell Biol.* 2016;18:1173-1184.
23. Liang JR, Lingeman E, Luong T, et al. A genome-wide ER-phagy screen highlights key roles of mitochondrial metabolism and ER-resident UFMylation. *Cell.* 2020;180, 11601-1177.
24. Zhou Z, Liu J, Fu T, et al. Phosphorylation regulates the binding of autophagy receptors to FIP200 Claw domain for selective autophagy initiation. *Nat Commun.* 2021;12:1570.
25. Fitzgerald KA, McWhirter SM, Faia KL, et al. IKK ϵ and TBK1 are essential components of the IRF3 signaling pathway. *Nat Immunol.* 2003;4:491-496.
26. Liu YP, Zeng L, Tian A, et al. Endoplasmic reticulum stress regulates the innate immunity critical transcription factor IRF3. *J Immunol.* 2012;189:4630-4639.
27. Maejima Y. The critical roles of protein quality control systems in the pathogenesis of heart failure. *J Cardiol.* 2020;75:219-227.
28. Maejima Y, Usui S, Zhai P, et al. Muscle-specific RING finger 1 negatively regulates pathological cardiac hypertrophy through downregulation of calcineurin A. *Circ Heart Fail.* 2014;7:479-490.
29. Usui S, Maejima Y, Pain J, et al. Endogenous muscle atrophy F-box mediates pressure overload-induced cardiac hypertrophy through regulation of nuclear factor-kappaB. *Circ Res.* 2011;109:161-171.
30. Kaizuka T, Morishita H, Hama Y, et al. An autophagic flux probe that releases an internal control. *Mol Cell.* 2016;64:835-849.
31. Hescheler J, Meyer R, Plant S, Krautwurst D, Rosenthal W, Schultz G. Morphological, biochemical, and electrophysiological characterization of a clonal cell (H9c2) line from rat heart. *Circ Res.* 1991;69:1476-1486.
32. Delorme-Axford E, Popelka H, Klionsky DJ. TEX264 is a major receptor for mammalian reticulophagy. *Autophagy.* 2019;15:1677-1681.

KEY WORDS autophagy, CCPG1, doxorubicin, endoplasmic reticulum

 **APPENDIX** For an expanded methods section and supplemental video, tables, and figures, please see the online version of this paper.